Dark-rearing uncovers novel gene expression patterns in an obligate cave-dwelling fish

Connor R. Sears, **Tyler E. Boggs**, **Joshua B. Gross**[*]

Department of Biological Sciences, University of Cincinnati, Cincinnati, OH 45221

Abstract

Extreme environments often result in the evolution of dramatic adaptive features. The Mexican tetra, *Astyanax mexicanus*, includes 30 different populations of cave-dwelling forms that live in perpetual darkness. As a consequence, many populations have evolved eye loss, reduced pigmentation, and amplification of non-visual sensory systems. Closely-related surface-dwelling morphs demonstrate typical vision, pigmentation, and sensation. Transcriptomic assessments in this system have revealed important developmental changes associated with the cave morph, however they have not accounted for photic rearing conditions. Prior studies reared individuals under a 12:12 hr light/dark (LD) cycle. Here, we reared cavefish under constant darkness (DD) for 5+ years. From these experimental individuals, we performed mRNA sequencing and compared gene expression of surface fish reared under LD conditions to cavefish reared under DD conditions to identify photic-dependent gene expression differences. GO enrichment analyses revealed a number of previously underappreciated cave-associated changes impacting blood physiology and olfaction. We further evaluated the position of differentially expressed genes relative to QTL positions from prior studies, and found several candidate genes associated with these ecologically relevant lighting conditions. In sum, this work highlights photic condition as a key environmental factor impacting gene expression patterns in blind cave-dwelling fish.

Graphical Abstract
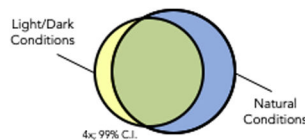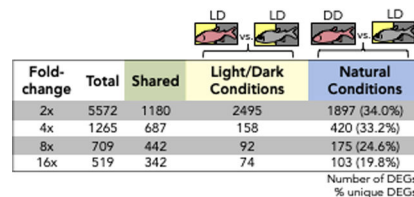
Keywords

RNA-seq; Mexican tetra; troglomorphy; regressive evolution

[*]*Corresponding author:* Joshua B. Gross, 312 Clifton Court, 711B Rieveschl Hall, Cincinnati, Ohio 45221; grossja@ucmail.uc.edu; Phone: 513-556-9708.

INTRODUCTION

Dramatic environmental shifts can have equally dramatic impacts on an organism's phenotype. These extreme changes can impact behavioral (Dall et al. 2012), morphological (Temerin and Cant 1983) or pigmentation phenotypes (Greenwood et al. 2011). However, these divergent phenotypes are often accompanied by changes at the molecular level, i.e. alterations to genetic regulation or structure (Carroll 2008, West-Eberhard 2003, Hoekstra et al. 2006), effectively linking the environment with the genomic and transcriptomic architectures. While taking many forms, deciphering this connection has been a key challenge in contemporary biological research. One increasingly utilized model to examine this link is the blind Mexican cavefish, *Astyanax mexicanus*. This species exists in two distinct morphotypes – a surface morph and cave-adapted morphs, found naturally in 30 distinct populations. Despite substantial similarities in their genomes, embryonic development, and geographic origin, these animals demonstrate very different phenotypes. The extant surface morphotype inhabits rivers and streams surrounding the Sierra de El Abra cave system of northeastern Mexico. Cavefish reside amidst a complex series of limestone caves in this region, and have evolved a number of "regressive" traits (Protas *et al.* 2006; Jeffery 2009a; Duboué *et al.* 2011), including the loss of eyes and a reduction of melanic pigmentation (ado lu 1957; 1967; Jeffery 2001; 2008; Yamamoto *et al.* 2003; Wilkens 2007), as well as "constructive" traits such as the expansion of non-visual sensory systems (Hassan 1989; Yoshizawa *et al.* 2014).

Despite these phenotypic differences, cave and surface morphs are members of the same species owing to their high genetic similarity and ability to interbreed to produce viable offspring (ado lu 1957; Avise and Selander 1972). Robust differences in gene expression (e.g., *shh, twhh,* and *pax6*) accompany many of the well-known phenotypic differences between the two morphotypes (Strickler *et al.* 2001; Yamamoto *et al.* 2003; Retaux *et al.* 2008; Pottin *et al.* 2011). Previous transcriptomic studies in this system capitalized on the genetic similarity between cave and surface fish to characterize genome-wide differential gene expression (Gross *et al.* 2013), eye loss (Hinaux *et al.* 2013) and convergent embryonic expression patterns (Stahl and Gross 2017).

Importantly, caves are characterized by a number of selective forces, including low food resources and absence of light (Elliott 2015; Jeffery 2015). Despite this absence of light, prior transcriptomic studies were carried out on cavefish reared under a 12:12 LD schedule. However, darkness is known to influence a number of regressive characters (Gonzalez and Aston-Jones 2008; Emerling and Springer 2014), such as downregulation of phototransduction genes in the Chinese cavefish, *Sinocyclocheilus anophthalmus* (Meng *et al.* 2013).

Mexican cavefish respond to light, despite the fact that most populations live in complete darkness and lose eyes through development. This light-sensing ability occurs through the pineal gland (Axelrod 1974; Yoshizawa and Jeffery 2008), and, bright light causes structural changes to photoreceptor cells of the pineal gland (Omura 1975). Conversely, surface fish raised in total darkness have smaller retinas, and their eyes appear darker owing to less

guanine deposition (Wilkens 1988; Gross *et al.* 2016), and they lose normal shoaling behaviors (Gregson and Burt de Perera 2007). When cavefish are reared in their natural photic conditions (constant darkness), they show very different motor activity and tank usage compared to those reared in light-dark conditions (Carlson and Gross 2018). Therefore, despite its effect on diverse phenotypes in *Astyanax*, the effect of light on gene expression has not yet been characterized in this system.

Here we present a transcriptomic analysis of cavefish and surface fish reared under two photic conditions each, constant darkness (DD) and a diurnal light/dark photoperiod (LD). Our interests centered mainly on the contrasts in gene expression under "natural" photic conditions, i.e. between cavefish reared in constant darkness and surface fish reared under light/dark conditions. Cavefish and surface fish demonstrate measurable behavioral differences under different lighting conditions (Carlson et al., 2018). Therefore, we predicted that this analysis would uncover numerous ecologically-relevant gene expression changes that would otherwise go unnoticed in studies that do not account for lighting condition. We found that gene expression differences did not simply reflect an expansion of previously established differences, but rather we found novel patterns associated with these normative lighting regimes. This work, which examines lighting as an essential regulator of gene expression, enables a clearer understanding of the interaction between genotype, phenotype, and environment in this fascinating natural model system.

METHODS

Animal Rearing

All experimental animals were maintained under identical light-dark (LD) or constant darkness (DD) rearing conditions. Our approach was to perform comprehensive RNA-sequencing of four conditions (two morphotypes under two lighting regimes) and perform pair-wise comparisons to examine how light impacts gene expression in cave and surface fish. Under the LD routine, animals experienced light within the room (494.62 ± 28.43 Lux) for 12 hours between 8:00am to 8:00pm (EST), followed by darkness (0.034 ± 0.007 Lux) for 12 hours. All light measurements were performed using an LT300 light meter (Extech Instruments, Nashua, NH). All fish were maintained in 5-gallon glass tanks with continuous flow of conditioned water (pH = 7.4 ± 0.2, conductivity = ~800 μS/cm; Aquaneering, San Diego, CA). All fish were maintained on a diet of flake food (TetraMin Pro). A subset of Pachón cavefish and surface fish embryos (>12 hours post-fertilization) were reared under dark-dark (DD) conditions for over five years. Animals were dark-reared in 5-gallon glass tanks wrapped in impermeable black construction paper. While the light level in LD tanks averaged 48.59 ± 6.32 lux, the DD tanks measured an average of only 0.27 ± 0.06 lux. This difference in illumination inside tanks is likely due to presence of shadows, which are a function of the physical placement of the tanks within our husbandry facility. We still observed a ~180-fold difference in light intensity between the LD and DD conditions, irrespective of tank placement within the husbandry facility. All other variables were held constant between LD and DD tanks and individuals. These experiments were conducted in compliance with the University of Cincinnati Institutional Animal Care and Use Committee (Protocol # 10-01-21-01).

RNA Isolation, Sequencing and Processing

RNA-sequencing was conducted on (n=4) adult individuals from each of the following groups: LD-reared surface fish (S^{LD}), DD-reared surface fish (S^{DD}), LD-reared cavefish (C^{LD}) and DD-reared cavefish (C^{DD}), for a total of 16 biological samples. All individuals were ~ five-years-old at the time of RNA extraction. We evaluated two lab-reared populations of *Astyanax mexicanus* originating from the Sierra de El Abra region of Mexico. These included individuals from the Pachón cave (pedigree 138) in Tamaulipas, Mexico; and surface-dwelling fish (pedigree 155) from the Río Sabinas and Río Valles drainages near Ciudad Valles, Mexico. Fish were originally obtained and generously provided to us by Dr. Richard Borowsky (NYU). Approximately four clutches of each morphotype were divided in half and randomly assigned to each lighting condition. RNA extractions were performed between 11am and 2pm (EST) to minimize variation associated with circadian patterns of gene expression (Idda *et al.* 2012). RNA extractions were performed under red-light illumination for DD individuals. Whole RNA isolation was performed separately for head and flank tissues, processed immediately using liquid nitrogen for tissue homogenization, and carried out using the RNeasy Universal Mini Kit according to the manufacturer instructions (Qiagen, Germantown, MD). Each sample was quality-assessed using a spectrophotometer, and samples were then pooled together and submitted to a sequencing core. Owing to our approach of pooling samples, we acknowledge the possibility that certain gene expression differences between cave and surface fish may arise as a simple consequence of presence/absence of certain structures (e.g., such as the eye). Having said this, the absence of certain vision-related genes can also serve as an important control for gene expression and GO enrichment analyses given our prior demonstration of reduced expression of vision-related genes in cave morphs (Gross et al., 2013). Samples were stored at −80°C prior to library synthesis and sequencing.

All RNA samples were then subjected to QC analysis (RQN>7) at the Cincinnati Childrens DNA Sequencing Core. Libraries were generated using only the pooled RNA extracts of head tissue, with the Illumina TruSeq 2 Poly-A stranded tail kit and sequenced as paired-end, 75bp reads to a depth of 10 million reads per sample (Illumina HiSeq 2500). Raw fastq-formatted reads were assessed using FastQC (v0.11.5) and filtered to remove TruSeq3-PE adapter sequences, trimmed for low quality leading- and trailing-bases below a quality measure of 3 (sliding window 4–15), and read lengths less than 36 bp (Trimmomatic software; Bolger *et al.* 2014). Following trimming, FastQC analyses were performed again to confirm removal of adapter and poor-quality sequences.

Differential Expression Analyses

Reads were aligned to the draft cavefish genome (v.93, ensembl.org) using ArrayStar (v15.0, DNAStar, Madison, WI). Each of our pooled samples was subjected to high-throughput sequencing as technical triplicates. Following alignment, we grouped all sequencing runs according to triplicate group and photic condition in order to evaluate within-sample variations across different sequencing runs. Normalized expression (RPKM; Mortazavi *et al.* 2008) was calculated for each experimental group: C^{LD}, S^{LD}, C^{DD} and S^{DD}. Expression similarity was quantified based on a global correlative value between experimental groups (Fig. 1). "Natural Conditions" refers to the comparison of C^{DD} and S^{LD} (Fig. 1C), and

"Light/Dark Conditions" refers to comparisons between C^{LD} and S^{LD} (Fig. 1B). The number of differentially expressed genes (DEGs) were determined by fold-change and confidence interval thresholds, and all DEG numbers were reported at a 99% confidence interval (Fig. 2; 3A). Genes that were deemed sensitive to lighting condition were based on differences in fold-change between natural conditions and light/dark conditions. The fold-change cutoff reported in Table 1 was generated based on a 2.5x threshold in C^{DD} and S^{LD}.

qPCR Validation

We assessed the expression of 16 genes demonstrating diverse patterns of expression by morphotype and lighting conditions, based on RNA-sequencing results (Figure S2). qPCR validation was carried out using a BioRad CFX96 real time PCR instrument (Hercules, California). RNA isolates from each treatment group (S^{LD}, S^{DD}, C^{LD} and C^{DD}) were used to generate cDNA. 1μg of RNA was thawed and annealed with 0.25μg of Oligo(dT)$_{12-18}$ Primer (Invitrogen) at 65°C for 10 minutes (C1000 Thermocycler, BioRad). To this preparation, we added 4μL of 5X Transcriptor RT reaction buffer (Millipore-Sigma), 0.5μL Protector RNase Inhibitor (Millipore-Sigma), 2μL dNTP mix (10 mM; Roche), and 0.5μL Transcriptor Reverse Transcriptase (Millipore-Sigma), and reactions were incubated at 50°C for 60 min, followed by inactivation of RT enzyme at 85°C for 5 minutes. cDNA preps were then stored at −20°C until use.

Amplifications were carried out using SsoFast EvaGreen Supermix (BioRad, Hercules, CA). Cycling conditions were: 1) activation: 95°C for 30s, 2) denaturation: 95°C for 5s, 3) annealing: 60°C for 5s, for 35 cycles, with 4) the addition of a melt curve: 65–95°C in 0.5°C increments of 5s/step. Normalized expression was calculated using the housekeeping gene *bactin1 (actb1*; ENSAMXG00000004264.1; McCurley and Callard 2008) using CFX Maestro software (v.4 BioRad, Hercules CA). Primers used for qPCR were blasted against the *Astyanax* reference genome, and confirmed to harbor a single match to the gene of interest using Primer-BLAST (NCBI, Primer3, Ye *et al.* 2012). Further, all amplicons demonstrated a single melt temperature, indicating the absence of multiple amplicons via qPCR analyses. Correlations between RNA-seq (RPKM) and qPCR expression values (C_t) were determined using Pearson's correlation test (MS Excel). The following primers were used for qPCR validation: *atp5pd* forward 5′-CGGTCCGCTAGGTGTCAGTA-3′, reverse 5′-TACCAAACCGCTGCAGAGAC-3′; *bactin1* forward 5′-ACACTGACATGTTGAACCCAA-3′, reverse 5′-ACCATGCAGCAGGATAAACATTG-3′; *cebpb* forward 5′-CAAAGGCAAGAAGCGCCTG-3′, reverse 5′- CATCTTGGCTTTATCGCGGC-3′; *col10a1b* forward 5′- TGCACAAGGTGTCTCATGCTA-3′, reverse 5′-CAGGCCTGGAGACCAAAGAA-3′; *ddit4* forward 5′-GACAGATGCTATTCTGTCAACTGC-3′, reverse 5′- AGCTGCCACAGCAAGTTTC-3′; *f8* forward 5′- GCAGTGAAGCCGCCTACAAA-3′, reverse 5′-GATGAATCGGGTGAATGCGG-3′; *hbz* forward 5′- TGGGACCTCTTCTGGGGTTA-3′, reverse 5′- TCTGCGTCTTCTCAACTCAGG-3′; *nfil3–5* forward 5′-GTCCAACAGTGGTACCCAGG-3′, reverse 5′- CTGTGTGACAGCCAGGTAGG-3′; *nfil3–6* forward 5′- GGAAATTCCTGAAGGCATGA-3′, reverse 5′-ACCGATAGGCTGCAGTTGAC-3′; *olfml3a* forward 5′-

CGAGCATCCGAGCCATGAAG-3′, reverse 5′- TACAGGGTGTCCTCGGACGTT-3′; *opn1w1* forward 5′- GTCTAATCCAGCCCAGGCAT-3′, reverse 5′- CTGCCTGTCGTCAAAGGAGC-3′; *rgs2* forward 5′- GACCTGCGAAGAGTTTCGAC-3′, reverse 5′- TCGGCGACTGACTCTTGATG-3′; *rho* forward 5′- TCACCATCGAGCACAAGAAG-3′, reverse 5′- CGAAGACGAAGTAGCCGTTC-3′; *rps18* forward 5′- ACACGAACATCGATGGTAGGAG-3′, reverse 5′- TTGTTGAGGTCGATGTCTGC-3′; *serpinh1b* forward 5′- CTCGGAGGAAAGTCGTCCAC-3′, reverse 5′- TCAGAAGCTCGGACAAACCC-3′; *smtlb* forward 5′- TGCACCTCCAACATCTTCCC-3′, reverse 5′- CCACCAGGGGATCAATCCAG-3′.

Gene Ontology Enrichment Analyses

Gene ontology (GO) enrichment analyses were performed using Blast2GO v.5 (Ashburner *et al.* 2000; Harris *et al.* 2004). The complete transcriptome predicted from the *Astyanax* genome (25,271 genes) was used as the GO terminology reference set. We generated a local database from the *Danio rerio* proteome using Blast2GO, which was obtained from the UniProt-Proteomes Database (UniProt ID: UP000000437). Pairwise GO enrichment analyses were performed for genes expressed at a 4-fold or higher difference.

QTL Comparison

QTL identified from prior studies (Borowsky and Wilkens 2002; Protas *et al.* 2007; Protas *et al.* 2008; Yoshizawa *et al.* 2012; O'Quin *et al.* 2013; Kowalko *et al.* 2013a; b; Gross *et al.* 2014) were localized to the current draft of the *Astyanax* genome (NCBI; McGaugh *et al.* 2014) through routine BLAST searches of the closest linked marker to each locus. Blast2GO was used to compare Ensembl and NCBI databases to the *Danio rerio* UniProt Database (UniProt ID: UP000000437). We used this resource to determine the chromosomal position of the *Astyanax* Ensembl database relative to the estimated chromosomal positions in the NCBI draft *Astyanax* genome. Prior analyses identified the genes *pmela* and *tyrp1b* as mediators of melanophore number in *Astyanax* cavefish (Stahl *et al.* 2018). As a proof-of-concept, we successfully retrieved the location of these genes in the current draft of the *Astyanax* genome (NCBI, Astyanax 2.0, v.102), using their associated QTL markers.

To identify candidate genes for eye loss, all genes with a known chromosomal position, a known QTL, and an expression difference of 2-fold or higher between cave and surface (under any lighting regime) were considered. 268 vision-related genes were selected with GO terms inclusive of 'eye', 'lens', 'visual', and 'retina' were included. 61 pigmentation-related genes with GO terms including the words 'chromophore', 'melanocyte', 'melanosome', 'melanin', or 'pigmentation' were included. Positional information for QTL (relative to selected candidate genes) was visualized using Circos (Fig. 4; Krzywinski, *et al.* 2009).

RESULTS

Alternate photic conditions reveal light-sensitive gene expression in *Astyanax*

We compared gene expression of all fish (i.e., both cave and surface) reared under LD-conditions to those reared under DD conditions, and observed a high correlation (R^2=0.9751; Figure 1A; Table S1). We then evaluated expression of all grouped cavefish data (irrespective of lighting condition) to all surface fish individuals and observed a slightly lower correlation (R^2=0.8873; Table S1). When examining expression patterns between cave and surface fish reared under light/dark conditions ($C^{LD} \times S^{LD}$), the correlative value dropped further (R^2=0.8657; Figure 1B; Table S1). The lowest correlation of global expression, however, was observed when we compared "natural conditions", i.e., gene expression in cavefish reared in darkness and surface fish reared under an LD photic regime ($C^{DD} \times S^{LD}$; R^2=0.8597; Figure 1C; Table S1). This suggests that global expression is *least* similar under photic regimes mimicking the natural conditions in which cave and surface morphs reside.

We next sought to understand the polarity of differential gene expression, to determine if a pattern exists with respect to over- and under-expressed genes in cavefish compared to surface fish. We found that at several fold-change thresholds (2-, 4-, 8-, or 16-fold), more genes are overexpressed in surface fish compared to cavefish (Fig. 2). For instance, considering genes displaying 4x fold change under LD photic conditions, 621 genes demonstrate lower expression values in C^{LD} compared to 224 genes with lower expression in S^{LD}. When comparing "natural" photic conditions, 785 genes are expressed at lower levels in C^{DD} compared to 322 genes demonstrating lower expression in S^{LD} (Fig. 2). As reported in prior studies (Stahl and Gross, 2017) the transcriptome reflects the pattern of more genes with lower expression in cavefish compared to surface fish, under light/dark and natural photic conditions.

These expression results are bolstered by a strong correlation (mean Pearson's coefficient = 0.868) between RNA-seq expression and qPCR analysis (Table S2; Fig. S2). Within our test group, five genes exhibited a correlative value > 0.95.

"Natural" photic rearing reveals novel differences in gene expression

We reasoned that rearing cave and surface fish under photic conditions that more closely mimic their natural photic environments would reveal gene expression differences not captured in prior studies. We began by analyzing expression differences at multiple fold change thresholds (2-, 4-, 8- and 16-fold) to compare transcriptomic responses under different lighting conditions (Fig. 3A). Interestingly, a significant number of the same genes were differentially expressed in both lighting conditions ("shared"; Fig. 3A). At each threshold, we discovered a number of differentially expressed genes that were only present when evaluating natural photic conditions. At a 2-fold threshold, 1897 genes were differentially expressed uniquely under natural photic conditions. This represents 34% of the DEGs at this threshold. At thresholds of 4-, 8- and 16-fold, at least 20% of genes were differentially expressed only in natural conditions. In total, 8065 genes were differentially expressed at 2-fold or higher, of which 2595 genes were uniquely identified under natural

photic conditions (> 32%). In sum, rearing *Astyanax* under natural photic conditions uncovered a considerable number of DEGs not observed in LD transcriptomic analyses.

To understand the novel changes to the transcriptome under natural photic conditions, we selected the most differentially-expressed genes in C^{DD} compared to S^{LD} (Table 1). Interestingly, we found that fold-change differences always increased in magnitude under "natural" conditions compared to light/dark conditions (Table 1), underscoring the importance of light in certain gene expression patterns.

Of the genes demonstrating the largest expression differences, several were associated with commonly-studied traits of cave animals including pigmentation and metabolism. One gene known to affect pigmentation is *gja5*, which encodes a gap junction protein belonging to the connexin family. Djurdjebi et al. 2019 hypothesized that *gja5* could be influential to forming a spotted pattern in brown trout by facilitating communication between multiple erythrophores, or between erythrophores and melanophores. A second gene implicated metabolism, *apoa1*, is linked to multiple human diseases, such as cardiovascular and early-onset nonfamiliar Alzheimer's disease, owing to its role in lipid metabolism (Lai et al. 2005; Vollbach et al. 2005).

At least eight of these genes influence blood physiology – an understudied system within cave animals. These genes can be categorized into two groups: hemoglobin production and detoxification/immunological function. Genes involved in detoxification and immunology displayed elevated expression in S^{LD} compared to C^{LD}, and even higher expression compared to C^{DD}. Two genes, *fgb* and *fgg*, are well known for their contributions to specific subunits of fibrinogen proteins. This protein can be converted to fibrin – which plays a key role in blood clotting. Additionally, *serpina1* and *hpx* maintain the highest patterns of expression in S^{LD} followed by C^{LD}, and then C^{DD}. *Serpina1* encodes serpin proteins, which inhibit enzymes playing a key role in inflammation, thrombosis and the complement cascade (Gooptu and Lomas 2008). *Hpx* encodes hemopexin, a glycoprotein with a high affinity for free hemoglobin, acting as an antioxidant following blood heme overload. Interestingly, all four of these genes were identified by Jima *et al.* (2009) as upregulated in mutant zebrafish that show signs of an "enhanced" innate immune response, to compensate for a lack of an effective adaptive immune system.

Four additional hemoglobin (*hbaa1, hbae1, ba1* and *hbaa2)* genes were highly differentially expressed in this analysis. Unlike the detoxification/immunological genes, these genes were expressed highest in C^{DD}, followed by C^{LD} and S^{LD}. This result was surprising in light of historic reports suggesting photic condition does not contribute to hemoglobin production or concentration. Hollwich (1979) and Robscheit-Robbins (1929) described experiments involving a range of taxa (horses, mules, humans, dogs, rabbits, roosters, frogs, fish) that displayed no long-term hematological changes in response to dark rearing. However, these studies were limited to animals with lineages of constant exposure to light, and were not introduced to darkness immediately following birth or fertilization.

To determine if the photic conditions we assessed were associated with functional shifts in gene expression, we performed a series of Gene Ontology (GO) enrichment analyses. We

began with an analysis of genes demonstrating higher expression in cavefish under LD conditions (compared to cavefish under DD conditions), and found enrichment of terms associated with olfaction (Figure S1). Unsurprisingly, genes expressed higher in S^{LD} compared to C^{LD} were associated with pigmentation, metabolism, and vision (Fig. S1). When comparing S^{LD} to C^{DD}, an unexpected category of terms was identified, blood physiology (Fig 3B). Genes with higher expression levels in cavefish reared in darkness were associated with pathways such as "oxygen transport", "oxygen binding" and "hemoglobin complex." Further, genes with reduced expression levels in C^{DD} were similarly associated with blood physiology, but in pathways associated primarily with blood coagulation. In sum, cave and surface fish reared under their natural photic regimes revealed a functional enrichment for genes involved in blood physiology (specifically associated with *hemoglobin* genes).

Olfaction also appears to be impacted by darkness, based on the enrichment of GO terms 'olfactory receptor activity' and 'response to odorant' in overexpressed genes in C^{DD} compared to C^{LD} (Figure 3B). Although these terms are also enriched in C^{LD} individuals, additional olfaction-related genes have a higher expression in C^{DD} relative to their light-dark reared counterparts. This suggests cavefish olfaction is sensitive to lighting condition, including particular odorant receptor genes expressed in olfactory neurons (Vogt *et al.* 1997; Alioto and Ngai 2005; Figure 3B). Olfactory receptor genes demonstrating a higher expression in cavefish include *or101–1*, *or118–2* (higher expression in C^{LD} compared to S^{LD}; data not shown). This pattern is repeated in C^{DD} compared to S^{LD} fish (e.g. *or126–1, or125–5*; higher expression in C^{DD} compared to S^{LD}).

Novel DEGs map near previously discovered QTL associated with regressive loss

To determine if any of the DEGs we identified map near the position of QTL discovered in prior studies, we assessed the positions of the *most* differentially expressed genes in our datasets. We began with 15 markers from prior QTL studies associated with vision loss (Figure 4A, light orange boxes), and surveyed across our transcriptomic analysis. In total, we evaluated 268 vision-related genes (Figure 4A, black hash marks) with differential expression between cave and surface fish, and identified 18 genes as potential candidates for eye loss (Figure 4A, bold hash marks and text). Two of these genes are *gucy* family members, *gucy2d, gucy2f.* A third candidate, *pde6ha*, previously identified in a microarray analysis (Strickler and Jeffery, 2009), was localized to chromosome 13 of the *Astyanax* genome, residing ~1.6Mb from eye loss QTL marker 30C (Fig. 4A). We also found the gene *rx3*, which lies ~5 Mb from marker 55A on chromosome 14 (Fig. 4A), which was originally proposed as a candidate for eye loss following a genomic analysis (McGaugh *et al.* 2014). We propose that these three genes, identified based on differential response to lighting condition, represent promising candidates for a role in the genetic basis for vision loss in *Astyanax*.

We then mapped the genomic position for 61 pigmentation genes. We identified candidates associated with the position of 11 pigmentation-associated QTL (Fig. 4B), and as a proof-of-concept, co-analyzed the position and expression of two genes (*pmela* and *tyrp1b*) previously implicated in pigmentation loss in cavefish (Stahl *et al.* 2018). Interestingly, the

expression of these genes decreases slightly in cavefish under dark rearing (Figure 4B). Included among our findings were the genes *sox18*, *gja5*, and *rab32b*. Located ~5Mb upstream of marker 206A (Figure 4B), *rab32b* is expressed 9.34-fold higher in C^{LD} fish compared to S^{LD} fish, and encodes a GTPase enzyme involved in membrane trafficking of tyrosinase and tyrosinase-related-protein between organelles in eukaryotic cells (Diekmann *et al.* 2011; Coppola *et al.* 2016; Braasch *et al.* 2009; Wasmeier *et al.* 2006). Although this gene is overexpressed in cavefish, downstream targets (*tryp1b*) are expressed at much lower levels (Stahl *et al.* 2018). However, we found a modest increase (1.24-fold) in *rab32b* expression in C^{DD} compared to S^{LD} fish (Figure 4B), suggesting this gene is mildly sensitive to light-dark conditions. The absence of light also affected the pigmentation-related gene, *gap junction protein 5b* (*gja5b*), which exhibits a 3.35-fold increase in expression in C^{DD} compared to S^{LD} (Table 1). Interestingly, this gene is expressed at similar levels in cave and surface fish reared on light/dark conditions (0.73 and 0.55 RPKM, respectively; Table 1). Based on their established roles in other systems, these three light-sensitive genes represent promising candidates for the complex genetic basis for pigmentation regression.

DISCUSSION

Dark-rearing reveals novel patterns of differential expression in the Mexican tetra

Previous studies in *Astyanax* characterized substantial variability in gene expression between cave and surface morphotypes (Gross *et al.* 2013; Hinaux *et al.* 2013). Many expression differences are rooted early in development, and likely contribute to phenotypic differences between cave and surface fish adults (Stahl and Gross 2017). Although these studies found several DEGs between cave and surface forms, the work we present here reveals that additional differences emerge when evaluating cavefish reared under their natural photic condition of complete darkness. We found that differential expression is mostly marked by under-expression in cavefish (Figure 2). Interestingly, this pattern of differential gene expression is not observed in transcriptomic analyses of development in cavefish compared to surface fish (Stahl and Gross 2017). In fact, the inverse appears to be true, with cavefish demonstrating a higher expression in more genes than surface fish; although, this pattern reverses as the embryos develop (Stahl and Gross 2017). The under-expression of certain genes in cavefish may indicate lower expression of certain genes contributes to trait regression.

Natural photic conditions reveal an effect of darkness on blood physiology and olfaction

We discovered that the transcription of several blood-related genes increases in darkness, including a number of *hemoglobin* genes (Table 1). Although the functional relevance and mechanism that underlies dark-dependent regulation of blood-related genes is unclear, one of the principle abiotic factors characterizing life in caves is reduced oxygen (Coineau 2000). The up-regulation of *hemoglobin* genes in C^{DD} likely evolved as an adaptation to reduced oxygen across the El Abra cave network (Ornelas-Garcia *et al.* 2018).

We noted a dramatic increase in expression of several *hemoglobin* subunits (*ba1*, *hbaa1*, *hbba2*, *hbae1.3*) exclusively in dark-reared cavefish (Table 1). A GO enrichment analysis revealed the terms "blood coagulation" and "fibrinogen" are enriched in down-regulated

genes of C^{DD} (Figure 3B). This is interesting since we observed a decrease in expression of two *fibrinogen* genes (*fgg* and *fgb*), which may mitigate blood clotting in light of increased hemoglobin concentration of blood (Table 1). This result contradicts historic literature. Sonnenlichtes (1919) suggested, "the belief that sunlight is indispensable to human welfare has become strongly entrenched in modern hygienic propaganda…it is therefore improbable that sunlight is in any sense directly concerned with the hematopoietic functions."

This discrepancy may also reflect an evolutionary adaptation evolving under intense environmental pressure. For instance, cavefish have lived in total darkness for thousands of generations, while animals in classic studies spent no more than a single generation in darkness. An alternative explanation could be phenotypic plasticity of *Astyanax*. Bilandžija *et al.* (2019) utilized dark-rearing, and found substantial plastic responses in this species, suggesting it may have facilitated successful recurrent colonization of epigean forms to the subterranean environment.

The enhancement to olfaction is less surprising. For instance, cavefish have an expanded telencephalon (wherein the olfactory bulbs are situated) compared to surface fish (Rétaux *et al.* 2008). It is unclear, however, why olfactory gene expression would be increased as a consequence of photic condition, but darkness may provide an environmental cue to increase the sensitivity of non-visual sensory systems (Yoshizawa *et al.* 2014).

Expression analyses reveal candidate genes for vision and pigmentation loss

Prior studies in *Astyanax* created hybrid pedigrees (ado lu 1957) permitting genetic studies of various cave-associated traits (Borowsky and Wilkins 2002) including pigmentation and eye loss (Gross *et al.* 2009; McGaugh *et al.* 2014; Stahl *et al.* 2018). We reasoned that our rearing paradigm could provide a source of additional candidate genes through co-analysis of expression data and positions of previously established QTL.

After reviewing several QTL studies (Borowsky and Wilkins 2002; Protas *et al.* 2007; Protas *et al.* 2008; Yoshizawa *et al.* 2012; O'Quin *et al.* 2013; Kowalko *et al.* 2013a; b; Gross *et al.* 2014), we compared positional information for 15 vision-related QTL (Fig. 4A). A putative role for certain candidate genes is illustrated by structural impacts in other species. For instance, defects in human *gucy2d* are linked to Leber's congenital amaurosis, a disorder of severe visual impairment caused by structural defects in the retina (Milam *et al.* 2003). Knockdown of *gucy2f* in zebrafish also causes visual impairment, accompanied by histological changes to the eye in *Danio* (Stiebel-Kalish *et al.* 2012). Further, both *gucy2d* and *gucy2f* are inactivated in subterranean-dwelling moles (*Heterocephalus glaber* and *Chrysochloris asiatica*; Emerling and Springer, 2014).

Another candidate gene, *pde6ha,* encodes a component of cone photoreceptors essential for phototransduction (Ionita and Pittler 2007; Collery and Kennedy 2010). Structural alterations to this gene in humans are associated with achromatopsia, an abnormality causing reduced visual acuity (Kohl *et al.* 2012). Although functional analyses of *pde6h* in mice did not cause noticeable changes in phototransduction (Brennenstuhl *et al.* 2015), in *Danio* this gene is upregulated in response to light (Weger *et al.* 2011).

We then mapped the genomic positions for 61 pigmentation genes, including *rab32b* (Figure 4B). Interestingly, in zebrafish embryos, *rab32* paralogs are expressed in the retinal pigment epithelium and developing melanoblasts (Coppola *et al.* 2016). Additionally, *Sox*-family transcription factors, such as *sox18,* regulate diverse events throughout early development, including neural crest migration (Kiefer 2007). *Sox18*-deficient mice have alterations to pheomelanin content in hair shafts, resulting in a darker appearance (Pennisi *et al.* 2000).

Another candidate gene we identified, *gja5,* is associated with human idiopathic atrial fibrillation, due to its role in activation of the atria (Gollob *et al.* 2006). In zebrafish, a mutation in *gja5b* is associated with the *leopard* mutant, which reorganizes stripe pigmentation into leopard-like spots (Irion *et al.* 2014). Taken together, the approach we use here illustrates the relevance of light as an environmental factor that likely impacts on quantitative changes in phenotype. This environmental factor is perhaps especially relevant for pigmentation, since cavefish harbor a number of coloration defects (Jeffery 2009b). Although neutral mutations may be an explanation for pigmentation loss, it is possible that secondary benefits arise with these specific mutations (Jeffery 2009b). For instance, genetic changes to key pigmentation genes may cause L-tyrosine (a melanin intermediate) to be blocked and shunted from its role in coloration, and utilized for L-dopamine production which in turn influence metabolism and foraging (Bilandžija et al., 2013). Future analyses of key environmental factors, such as photic condition, may further inform the adaptive nature of these complex interactions.

CONCLUSIONS

The blind Mexican cavefish has evolved under the pressure of constant darkness. Both genetic variation and plasticity play key roles in ecologically relevant traits. Although a captive laboratory environment provides exceptional control over numerous confounding variables, this work reveals that inclusion of key environmental variables (e.g., lighting condition) is essential for understanding the complex processes by which animals evolve in the wild. This study revealed that rearing under 'natural photic conditions' (darkness) yields substantially different gene expression patterns compared to light/dark rearing. Here, we report that dark-rearing impacts expression of suites of genes associated with well-known troglomorphic traits such as pigmentation reduction and vision loss. This work also revealed expression differences associated with less understood traits evolving in cavefish, such as blood physiology. Our expression analyses demonstrating labile expression associated with photic condition, alongside prior QTL studies, revealed additional candidate genes for eye or pigmentation loss. Moreover, this study indicates the importance of photic condition as an environmental pressure in the blind Mexican cavefish, and underscores the importance of accounting for natural lighting conditions when examining genetic and phenotypic expression in this system.

Supplementary Material

Refer to Web version on PubMed Central for supplementary material.

ACKNOWLEDGEMENTS

REFERENCES

Alioto TS, and Ngai J, 2005 The odorant receptor repertoire of teleost fish. BMC Genomics. 6: 173. [PubMed: 16332259]

Ashburner M, Ball CA, Blake JA, Botstein D, Butler H, et al., 2000 Gene Ontology: Tool for the unification of biology. Nature Genet. 25: 25–29. [PubMed: 10802651]

Avise JC and Selander RK, 1972 Evolutionary Genetics of Cave-Dwelling Fishes of the Genus *Astyanax*. Evolution. 26: 1–19. [PubMed: 28555764]

Axelrod J, 1974 The pineal gland: A neurochemical transducer. Science, 184: 1341–1348. [PubMed: 4151465]

Bilandžija H, Ma L, Parkhurst A and Jeffery WR. 2013 A potential benefit of albinism in *Astyanax* cavefish: Downregulation of the *oca2* gene increases tyrosine and catecholamine levels as an alternative to melanin synthesis. PLoS One, 8:11.

Bilandžija H, Hollifield B, Steck M, Meng G, Ng M, et al., 2019 Phenotypic plasticity as an important mechanism of cave colonization and adaption in Astyanax cavefish. bioRxiv 657460; doi: 10.1101/657460.

Bolger AM, Lohse M, and Usadel B, 2014 Trimmomatic: A flexible trimmer for Illumina sequence data. Bioinformatics 30: 2114–2120. [PubMed: 24695404]

Borowsky R, and Wilkens H, 2002 Mapping a cave fish genome: Polygenic systems and regressive evolution. J. Hered 93: 19–21. [PubMed: 12011170]

Braasch I, Brunet F, Volff JN, and Schartl M, 2009 Pigmentation pathway evolution after whole-genome duplication in fish. Genome Biol. Evol 1: 479–493. [PubMed: 20333216]

Brennenstuhl C, Tanimoto N, Burkard M, Wagner R, Bolz S, et al., 2015 Targeted ablation of *Pde6h* in mice reveals cross-species differences in cone and rod phototransduction protein inventory. J. Biol. Chem 290: 10242–10255. [PubMed: 25739440]

Carlson BM, and Gross JB, 2018 Characterization and comparison of activity profiles exhibited by the cave and surface morphotypes of the blind Mexican tetra, *Astyanax mexicanus*. Comp. Biochem. Physiol. C Toxicol. Pharmacol 208: 114–129. [PubMed: 28823830]

Carlson BM, Klingler IB, Meyer BJ and Gross JB, 2018 Genetic analysis reveals candidate genes for activity QTL in the blind Mexican tetra, *Astyanax mexicanus*. PeerJ. 6:e5189. [PubMed: 30042884]

Carroll SB, 2008 Evo-Devo and an expanding evolutionary synthesis: a genetic theory of morphological evolution. Cell. 134: 25–36. [PubMed: 18614008]

Coineau N, 2000 Adaptations to interstitial groundwater life, pp. 189–210 in Ecosystems of the World: Subterranean Ecosystems, edited by Wilkens H, Culver DC, and Humphreys WF. Elsevier Science B. V., Amsterdam.

Collery RF, and Kennedy BN, 2010 Photoreceptor guanylate cyclases and cGMP phosphodiesterases in zebrafish, pp. 55–61 in Retinal Degenerative Diseases. Advances in Experimental Medicine and Biology, vol. 664, edited by Anderson R, Hollyfield J, and LaVail M. Springer, New York.

Coppola U, Annona G, D'Aniello S, and Ristoratore F, 2016 *Rab32* and *Rab38* genes in chordate pigmentation: An evolutionary perspective. BMC Evol. Biol 16: 26. [PubMed: 26818140]

Dall ARX, Bell AM, Bolnickand DI and Ratnieks FLW, 2012 An evolutionary ecology of individual differences. Ecol. Lett 15: 1189–1198. [PubMed: 22897772]

Diekmann Y, Seixas E, Gouw M, Tavares-Cadete F, Seabra MC, et al., 2011 Thousands of rab GTPases for the cell biologist. PLoS Comput. Biol 7: e1002217. [PubMed: 22022256]

Djurdjevi I, Furmanek T, Miyazawa S, and Bajec SS, 2019 Comparative transcriptome analysis of trout skin pigment cells. BMC Genomics. 20:359. [PubMed: 31072301]

Duboué ER, Keene AC and Borowsky RL, 2011 Evolutionary Convergence on Sleep Loss in Cavefish Populations. Curr. Biol 8: 671–676.

Elliott WR, 2015 Cave biodiversity and ecology of the Sierra de El Abra region, pp. 59–75 in Biology and Evolution of the Mexican Cavefish, edited by Keene AC, Yoshizawa M, and McGaugh SE. Elsevier, San Diego.

Emerling CA, and Springer MS, 2014 Eyes underground: Regression of visual protein networks in subterranean mammals. Mol. Phylogenetics Evol 78: 260–270.

Gollob MH, Jones DL, Krahn AD, Danis L, Gong XQ, et al., 2006 Somatic mutations in the connexin 40 gene (*GJA5*) in atrial fibrillation. N. Engl. J. Med 354: 2677–2688. [PubMed: 16790700]

Gonzalez MMC, and Aston-Jones G, 2008 Light deprivation damages monoamine neurons and produces a depressive behavioral phenotype in rats. PNAS. 105: 4898–4903. [PubMed: 18347342]

Gooptu B, and Lomas DA, 2008 Polymers and inflammation: disease mechanisms of the serpinopathies. J. Exp. Med 7: 1529.

Gregson JNS and Burt de Perera T, 2007 Shoaling in eyed and blind morphs of the characin *Astyanax fasciatus* under light and dark conditions. J. Fish Biol 70: 1615–1619.

Greenwood AK, Jones FC, Chan YF, Brady SD, Absher DM, et al., 2011 The genetic basis of divergent pigment patters in juvenile threespine sticklebacks. Heredity. 107: 155–166. [PubMed: 21304547]

Gross JB, Borowsky R, and Tabin CJ, 2009 A novel role for *Mc1r* in the parallel evolution of depigmentation in independent populations of the cavefish *Astyanax mexicanus*. PLoS Genet. 5: e1000326. [PubMed: 19119422]

Gross JB, Furterer A, Carlson BM, and Stahl BA, 2013 An integrated transcriptome-wide analysis of cave and surface dwelling *Astyanax mexicanus*. PLoS ONE. 8: e55659. [PubMed: 23405189]

Gross JB, Krutzler AJ, and Carlson BM, 2014 Complex craniofacial changes in blind cave-dwelling fish are mediated by genetically symmetric and asymmetric loci. Genetics. 196: 1303–1319. [PubMed: 24496009]

Gross JB, Powers AK, Davis EM, and Kaplan SA, 2016 A pleiotropic interaction between vision loss and hypermelanism in *Astyanax mexicanus* cave x surface hybrids. BMC Evol. Biol 16: 145. [PubMed: 27363593]

Harris MA, Clark J, Ireland A, Lomax J, Ashburner M, et al., 2004 The Gene Ontology (GO) database and informatics resource. Nucleic Acids Res. 32: D258–261. [PubMed: 14681407]

Hassan ES, 1989 Hydrodynamic imaging of the surroundings by the lateral line of the blind cave fish *Anoptichthys jordani*, pp. 217–227 in The Mechanosensory Lateral Line, edited by Coombs S, Görner P, and Münz H. Springer, New York.

Hinaux H, Poulain J, Da Silva C, Noirot C, Jeffery WR, et al., 2013 *De novo* sequencing of *Astyanax mexicanus* surface fish and Pachón cavefish transcriptomes reveals enrichment of mutations in cavefish putative eye genes. PloS ONE. 8: e53553. [PubMed: 23326453]

Hoekstra HE, 2006 Genetics, development and evolution of adaptive pigmentation in vertebrates. Heredity. 97: 224–234.

Hollwich F, 1979 Light and Blood Count, pp 39–42 in The influence of ocular light perception on metabolism in man and in animal. Springer, New York.

Idda ML, Bertolucci C, Vallone D, Gothilf Y, Sánchez-Vázquez FJ, and Foulkes NS, 2012 Circadian clocks: Lessons from fish, pp. 41–57 in Progress in Brain Research. Elsevier, San Diego.

Ionita MA and Pittler SJ, 2007 Focus on molecules: rod cGMP phosphodiesterase type 6. Exp. Eye Res 84: 1–2. [PubMed: 16563379]

Irion U, Frohnhöfer HG, Krauss J, Champollion TC, Maischein HM, et al., 2014 Gap junctions composed of connexins 41.8 and 39.4 are essential for colour pattern formation in zebrafish. eLife. 3: e05125. [PubMed: 25535837]

Jeffery WR 2001 Cavefish as a model system in evolutionary developmental biology. Dev. Biol 231: 1–12. [PubMed: 11180948]

Jeffery WR, 2008 Emerging model systems in evo-devo: Cavefish and microevolution of development. Evol. Dev 10: 265–272. [PubMed: 18460088]

Jeffery WR, 2009a Evolution and development in the cavefish *Astyanax*. Curr. Top. Dev. Biol 86: 191–221. [PubMed: 19361694]

Jeffery WR 2009b Regressive evolution in *Astyanax* cavefish. Annu. Rev. Genet 43: 25–47. [PubMed: 19640230]

Jeffery WR, 2015 Pigment regression and albinism in *Astyanax* cavefish, pp. 155–174 in Biology and Evolution of the Mexican Cavefish, edited by Keene AC, Yoshizawa M, and McGaugh SE. Elsevier, San Diego.

Jima DD, Shah RN, Orcutt TM, Joshi D, McHugh Law J, et al., 2009 Enhanced transcription of complement and coagulation genes in the absence of adaptive immunity. Mol. Immunol 7: 1505–1516.

Kiefer JC, 2007 Back to basics: *Sox* genes. Dev. Dyn 236: 2356–2366. [PubMed: 17584862]

Kohl S, Coppieters F, Meire F, Schaich S, Roosing S, et al., 2012 A nonsense mutation in *PDE6H* causes autosomal-recessive incomplete achromatopsia. Am. J. Hum. Genet 91: 527–532. [PubMed: 22901948]

Kowalko JE, Rohner N, Linden TA, Rompani SB, Warren WC, et al., 2013a Convergence in feeding posture occurs through different genetic loci in independently evolved cave populations of *Astyanax mexicanus*. PNAS. 110: 16933–16938. [PubMed: 24085851]

Krzywinski MI, Schein JE, Birol I, Connors J, Gascoyne R, et al., 2009 Circos: an information aesthetic for comparative genomics. Genome Res. 19: 1639–1645. [PubMed: 19541911]

Lai CQ, Parnell LD and Jose M, 2005 The *APOA1/C3/A4/A5* gene cluster, lipid metabolism and cardiovascular disease risk. Curr. Opin. Lipidol 16: 153–166. [PubMed: 15767855]

McCurley AT and Callard GV, 2008 Characterization of housekeeping genes in zebrafish: male-female differences and effects of tissue type, developmental stage and chemical treatment. BMC. MOL. BIOL 9: 102. [PubMed: 19014500]

McGaugh SE, Gross JB, Aken B, Blin M, Borowsky R, et al., 2014 The cavefish genome reveals candidate genes for eye loss. Nat. Commun 5: 5307. [PubMed: 25329095]

Meng F, Braasch I, Phillips JB, Lin X, Titus T, et al., 2013 Evolution of the eye transcriptome under constant darkness in *Sinocyclocheilus* cavefish. Mol. Biol. Evol 30: 1527–1543. [PubMed: 23612715]

Milam AH, Barakat MR, Gupta N, Rose L, Aleman TS, et al., 2003 Clinicopathologic effects of mutant GUCY2D in Leber congenital amaurosis. Ophthalmology, 110: 549–558. [PubMed: 12623820]

Mortazavi A, Williams BA, McCue K, Schaeffer L, and Wold B, 2008 Mapping and quantifying mammalian transcriptomes by RNA-Seq. Nature Methods 5: 621. [PubMed: 18516045]

O'Quin KE, Yoshizawa M, Doshi P, and Jeffery WR, 2013 Quantitative genetic analysis of retinal degeneration in the blind cavefish *Astyanax mexicanus*. PloS ONE, 8: e57281. [PubMed: 23437360]

Omura Y, 1975 Influence of light and darkness on the ultrastructure of the pineal organ in the blind cave fish, *Astyanax mexicanus*. Cell Tissue Res, 160: 99–112. [PubMed: 1170953]

Ornelas-García P, Pajares S, Sosa-Jiménez VM, Rétaux S, and Miranda-Gamboa RA, 2018 Microbiome differences between river-dwelling and cave-adapted populations of the fish *Astyanax mexicanus* (De Filippi, 1853). PeerJ, 6: e5906.

Pennisi D, Gardner J, Chambers D, Hosking B, Peters J, et al., 2000 Mutations in *Sox18* underlie cardiovascular and hair follicle defects in ragged mice. Nature Genet. 24: 434–437. [PubMed: 10742113]

Pottin K, Hinaux H, and Rétaux S, 2011 Restoring eye size in *Astyanax mexicanus* blind cavefish embryos through modulation of the *Shh* and *Fgf8* forebrain organising centres. Development, 138: 2467–2476. [PubMed: 21610028]

Protas ME, Hersey C, Kochanek D, Zhou Y, Wilkens H, et al., 2006 Genetic analysis of cavefish reveals molecular convergence in the evolution of albinism. Nature Genet. 38: 107. [PubMed: 16341223]

Yoshizawa M, Yamamoto Y, O'Quin KE, and Jeffery WR, 2012 Evolution of an adaptive behavior and its sensory receptors promotes eye regression in blind cavefish. BMC Biol. 10: 108. [PubMed: 23270452]

Yoshizawa M, Jeffery WR, van Netten SM, and McHenry MJ, 2014 The sensitivity of lateral line receptors and their role in the behavior of Mexican blind cavefish (*Astyanax mexicanus*). J. Exp. Biol 217: 886–895. [PubMed: 24265419]
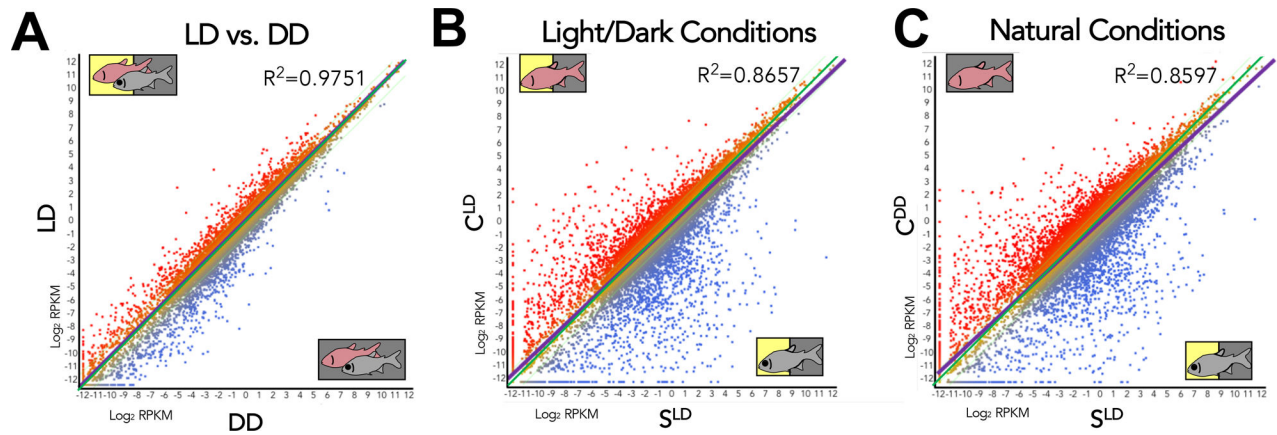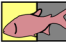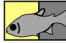
Figure 1. Correlations between morphotypes are least similar under natural conditions.
Each point on this scatterplot represents an individual gene. Some genes (red) have a higher expression in the condition on the y-axis. Other genes (blue) have a higher expression in the condition on the x-axis. LD vs. DD (A) is more similar than light/dark conditions (B), while natural conditions (C) are the least related based on the R^2 and spread of points about the line of regression (purple). As each of these scatterplots encapsulates all 25,271 genes, any visible changes correlate to large scale changes in global gene expression. The increasing distance between the line of regression (purple) and the zero-fold line (green) viewed between panels A to C yields an approximation of the increase in difference between the two conditions.

Condition	2-fold		4-fold		8-fold		16-fold	
	+	-	+	-	+	-	+	-
Natural Conditions DD vs. LD	1431	**1646**	322	**785**	133	**484**	93	**352**
Light/Dark Conditions LD vs. LD	776	**1092**	224	**621**	98	**436**	76	**340**

Number of DEGs

Figure 2. More genes are under-expressed in cavefish, regardless of rearing conditions.
Genes with a higher (plus) or lower (minus) expression in cavefish in comparison to surface fish under both natural and light/dark conditions reveal a higher number of genes with a lower expression in cavefish regardless of the lighting condition. This pattern may indicate that the function of many genes is reduced in the cavefish compared to the surface fish. The replication of this pattern in the dark indicates that this pattern of under-expression in cavefish is conserved regardless of lighting condition.
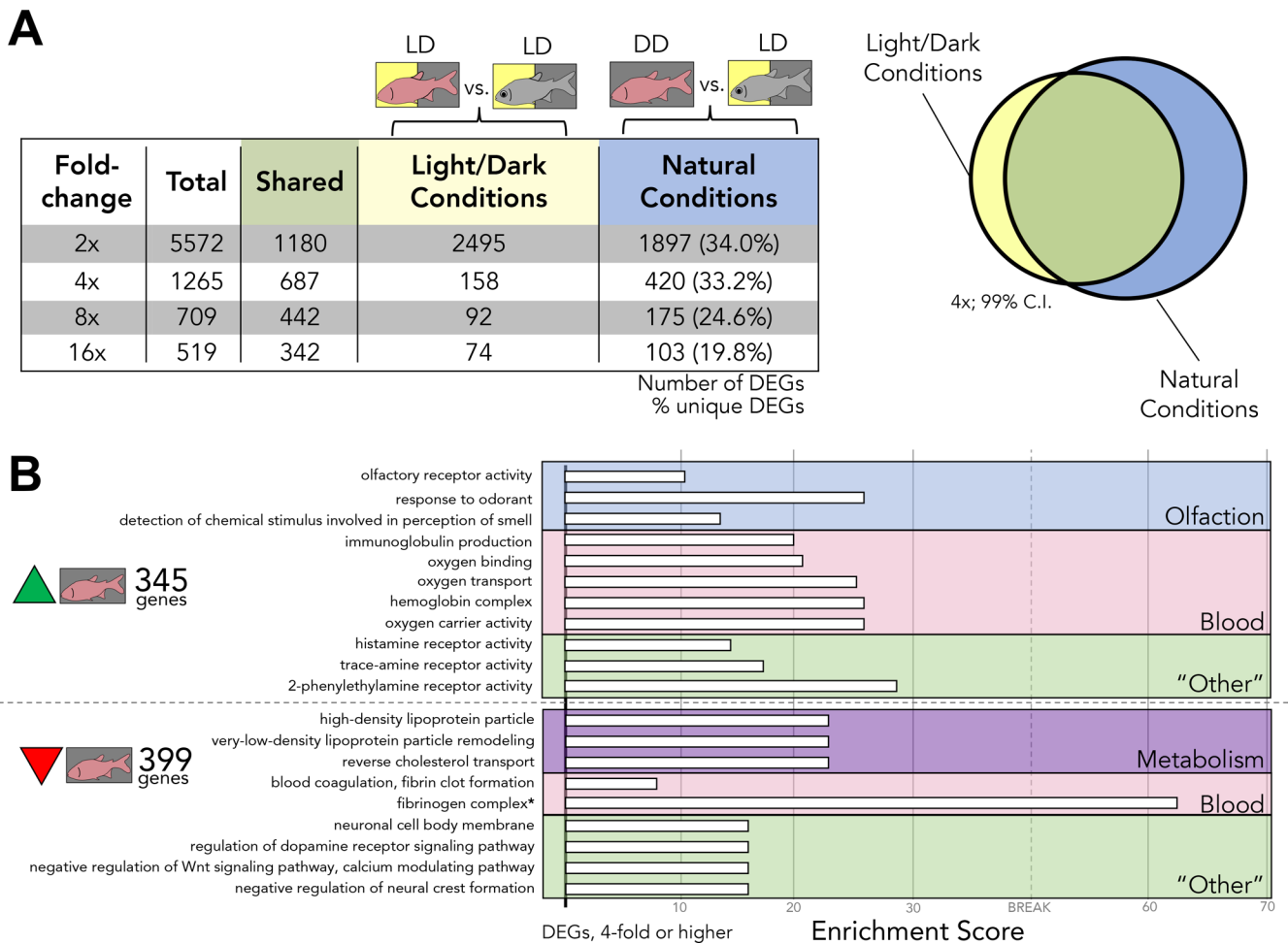
Figure 3. Rearing under natural photic conditions reveals novel changes to gene expression.
A) The number of differentially expressed genes unique to either light/dark conditions or natural conditions is represented in the 4th and 5th columns of the table, respectively. These DEGs are inclusive of genes with a higher expression in either cave or surface fish on their respective lighting conditions, represented diagrammatically to the right of the table (Venn diagram). There are a large number of differentially expressed genes that are revealed under natural conditions alone. This large number of DEGs represent a set of genes that have not been previously explored B) Test sets of genes were selected based on their expression at a 4-fold threshold. DEGs unique to natural conditions were assessed. Under light/dark conditions, 345 genes have a higher expression in C^{DD} compared to S^{LD} and 399 have a lower expression in C^{DD} compared to S^{LD}. The proportion of GO terms in these test sets was compared to the proportion of GO terms found in the whole transcriptome as a reference. The observed occurrence of each term is taken over the expected occurrence of each term based on is proportion in the reference. Each white bar to the right of a term represents an "Enrichment Score" (observed/expected). This indicates that dark-rearing may potentially play a role in the development and function of the circulatory, olfactory, and metabolic systems in *A. mexicanus* cavefish.

A

Gene ID	Symbol	Gene Function	S^LD RPKM	C^LD RPKM	C^DD RPKM
ENSAMXG00000000032.1	gucy2f	Zebrafish KOs affect retinal development	1.188	0.038	0.034
ENSAMXG00000017731.1	cryba1a	Cryba1 KO mice display retinal vessel defects	56.614	0.003	0.028
ENSAMXG00000001722.1	opn1lw1*	Defects in human gene can results in color blindness	57.765	0.133	0.176
ENSAMXG00000001577.1	crx	crx KOs display impaired vision and response to light	4.688	0.293	0.479
ENSAMXG00000008452.1	gucy2d	Zebrafish KOs display affected retinal development	0.932	0.032	0.026
ENSAMXG00000017182.1	exorh	Expressed in pineal gland; extraocular rhodopsin	1.398	0.301	0.25
ENSAMXG00000006082.1	guca1a	Associated with maculopathy in human	3.492	0.005	0.015
ENSAMXG00000014334.1	kera*	Mice KO affects corneal fiber organization and diameter	1.558	0.006	0.178
ENSAMXG00000002203.1	cryba2a	Causative factor of cataracts	23.956	0.023	0.016
ENSAMXG00000010786.1	pde6ha*	Functions in photoreceptor development	9.788	0.019	0.038
ENSAMXG00000015728.1	aanat1*	Functions in circadian regulation of sleep	2.524	0.169	0.057
ENSAMXG00000013352.1	gc2	Expressed in cone photoreceptors	3.151	0.022	0.019
ENSAMXG00000008320.1	rx3*	Critical for eye formation	0.308	0.003	0.012
ENSAMXG00000015083.1	rx2*	Necessary for retinal cell maintenance	1.55	0.002	0.002
ENSAMXG00000010509.1	rom1b*	KOs exhibit abnormal pigment growth in eye	32.492	0.012	0.056
ENSAMXG00000013651.1	rlbp1b	KOs exhibit delayed response to dark environment	8.459	0.242	0.203
ENSAMXG00000001987.1	ninl	Functions in photoreceptor development	1.064	0.406	0.551
ENSAMXG00000006671.1	znf503	Negative regulator of transcription; involved in eye morphogenesis	0.463	0.642	0.977

Vision-related QTL

B

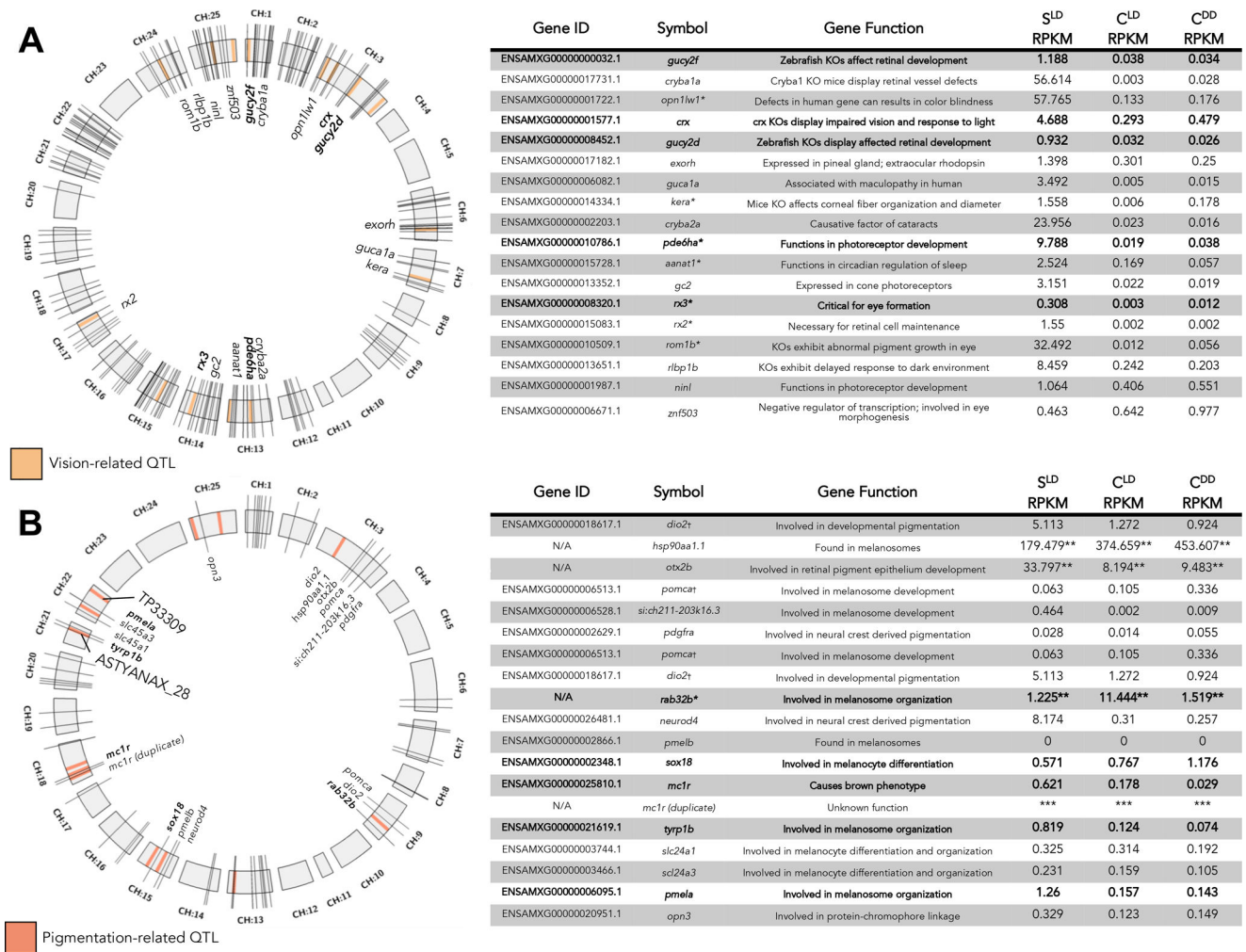| Gene ID	Symbol	Gene Function	S^LD RPKM	C^LD RPKM	C^DD RPKM
ENSAMXG00000018617.1	dio2†	Involved in developmental pigmentation	5.113	1.272	0.924
N/A	hsp90aa1.1	Found in melanosomes	179.479**	374.659**	453.607**
N/A	otx2b	Involved in retinal pigment epithelium development	33.797**	8.194**	9.483**
ENSAMXG00000006513.1	pomca†	Involved in melanosome development	0.063	0.105	0.336
ENSAMXG00000006528.1	si:ch211-203k16.3	Involved in melanosome development	0.464	0.002	0.009
ENSAMXG00000002629.1	pdgfra	Involved in neural crest derived pigmentation	0.028	0.014	0.055
ENSAMXG00000006513.1	pomca†	Involved in melanosome development	0.063	0.105	0.336
ENSAMXG00000018617.1	dio2†	Involved in developmental pigmentation	5.113	1.272	0.924
N/A	rab32b*	Involved in melanosome organization	1.225**	11.444**	1.519**
ENSAMXG00000026481.1	neurod4	Involved in neural crest derived pigmentation	8.174	0.31	0.257
ENSAMXG00000002866.1	pmelb	Found in melanosomes	0	0	0
ENSAMXG00000002348.1	sox18	Involved in melanocyte differentiation	0.571	0.767	1.176
ENSAMXG00000025810.1	mc1r	Causes brown phenotype	0.621	0.178	0.029
N/A	mc1r (duplicate)	Unknown function	***	***	***
ENSAMXG00000021619.1	tyrp1b	Involved in melanosome organization	0.819	0.124	0.074
ENSAMXG00000003744.1	slc24a1	Involved in melanocyte differentiation and organization	0.325	0.314	0.192
ENSAMXG00000003466.1	scl24a3	Involved in melanocyte differentiation and organization	0.231	0.159	0.105
ENSAMXG00000006095.1	pmela	Involved in melanosome organization	1.26	0.157	0.143
ENSAMXG00000020951.1	opn3	Involved in protein-chromophore linkage	0.329	0.123	0.149

Pigmentation-related QTL

Figure 4. Vision and pigmentation genes localized to previously identified QTL providing novel candidate genes.

The distribution of vision-related (A) and pigmentation-related (B) QTL (light orange or light pink boxes) across the 25 chromosomes of the draft *Astyanax* genome (gray boxes, CH:1–25). Gene identity and function are represented in the tables to the right. Values are given in RPKM (normalized expression). Some genes fall remarkably close to QTL (represented as bold hash marks and text) and demonstrate relevant alterations in development when function is disrupted in other systems. * indicates gene name was derived from *Danio rerio* based on sequence similarity. ** indicates RPKM was obtained via RNA-seq alignment to *Astyanax* NCBI draft genome by chromosome, and cannot be directly compared to other values, although intra-gene comparisons of expression based on morphotype and lighting condition are valid. † indicates an *A. mexicanus* gene that aligns to the same protein in *D. rerio* as another *A. mexicanus* gene by BLAST. *** is used in place of expression values for the duplicate *mc1r* gene due to incomplete functional and coding information for this copy number variant.

Table 1.

Genes identified with the greatest fold change difference when comparing surface fish and cavefish reared under their natural photic conditions (S^{LD} vs C^{DD}).

Gene	Gene Description	S^{LD} RPKM	C^{LD} RPKM	C^{DD} RPKM	LD Conditions Fold Change	Natural Conditions Fold Change
hbaa1	*Hemoglobin subunit alpha 1*	63.3	98.3	1337.4	1.6 up	21.1 up
adgre6	*Adhesion G protein-coupled receptor E6 (Fragment)*	0.2	1.7	2.3	9.9 up	13.6 up
hbae1.3	*Hemoglobin, alpha embryonic 1.3 (Fragment)*	0.2	1.1	2.5	5.4 up	11.8 up
ba1	*Hemoglobin subunit beta-1*	399.3	530.4	3996.7	1.3 up	10.0 up
faua	*40S ribosomal protein S30*	12.4	17.2	116.5	1.4 up	9.4 up
hbaa1	*Hemoglobin subunit alpha 1*	337.6	527.1	2828.7	1.6 up	8.4 up
ba1	*Hemoglobin subunit beta-1*	32.3	43.1	151.1	1.3 up	4.7 up
tnni2a.4	*Fast muscle troponin I*	26.9	70.7	117.6	2.6 up	4.4 up
gja5b	*Gap junction protein 5b*	0.6	0.7	1.8	1.3 up	3.4 up
hbba2	*Hemoglobin, beta adult 2*	585.5	1111.1	1527.1	1.9 up	2.6 up
ckbb	*Brain-subtype creatine kinase*	134.0	68.0	41.8	2.0 down	3.2 down
hpx	*Hemopexin*	530.1	329.8	151.2	1.6 down	3.5 down
apoa1	*Apolipoprotein A-I*	3891.5	2905.4	1057.4	1.3 down	3.7 down
slc25a48	*Solute carrier family 25 member 48*	2.1	1.8	0.5	1.2 down	4.0 down
serpina1	*Serpin peptidase inhibitor, clade A (alpha-1 antiproteinase, antitrypsin), member 1*	730.8	282.2	168.6	2.6 down	4.3 down
fgb	*Fibrinogen beta chain*	172.6	105.3	38.9	1.6 down	4.4 down
fgg	*Fgg protein*	177.3	91.3	35.1	1.9 down	5.1 down
abl2	*Tyrosine-protein kinase*	1.8	1.4	0.2	1.3 down	7.6 down
cebpb	*CCAAT enhancer-binding protein beta*	224.1	123.1	22.2	1.8 down	10.1 down
cebpd	*CCAAT enhancer-binding protein delta*	323.7	200.5	30.1	1.6 down	10.7 down